PHOTON SIGNATURES FOR STANDOFF BOMB DETECTION

by

KYLE W. LOSCHKE

B.S., Kansas State University, 2006

A THESIS

submitted in partial fulfillment of the requirements for the degree

MASTER OF SCIENCE

Department of Mechanical and Nuclear Engineering
College of Engineering

KANSAS STATE UNIVERSITY
Manhattan, Kansas

2008

Approved by:

Major Professor
Dr. William L. Dunn

Copyright

Abstract

The purpose of this research was to develop a technology to quickly identify hidden explosive materials. The developed method needs to be performed at a standoff distance of approximately two meters or more, must have high sensitivity (low false-negative rate) and good specificity (low false-positive rate), and should be able to detect a minimum amount of approximately one gallon (15 lbs) of explosive material.

In an effort to meet these goals, a template-matching procedure to aid in the rapid detection of hidden improvised explosive devices was investigated. Multiple photon-scattered responses are being used as a part of a multidimensional signature-based radiation scanning (SBRS) approach in an attempt to detect chemical explosives at safe, standoff distances. The SBRS approach utilizes both neutron and photon interrogation to determine if a target contains explosive material, but the focus of this thesis is on photon interrogation.

Beams of photons are used to create back-streamed responses called signatures, which are dependent on the density and the composition of the target. These signatures are compared to templates, which are collections of the same signatures if the interrogated volume contained a significant amount of explosives. The signature analysis produces a single figure-of-merit. A low figure-of-merit indicates an explosive might be present in the target. Experiments have been conducted that show an explosive surrogate (fertilizer) can be distinguished from several inert materials using these photon signatures, proving these signatures to be very useful in this particular method of chemical explosive detection.

Table of Contents

List of Figures

List of Tables

Acknowledgements

This research was funded through the award of a contract from the United States Marine Corps Systems Command to M2 Technologies, Inc. I would like to thank M2 Technologies for their generous support throughout my research. A very special thanks is due to Dr. William Dunn for his guidance and encouragement, and for giving me the opportunity to work on this standoff bomb detection project.

Dedication

This is for my parents, Frank and Raylene, for their never-ending support, generosity, and love.

CHAPTER 1 - Introduction

1.1 The Problem

The continuous growth of international travel and trade has led to an increase in the smuggling of weapons and illicit drugs. Over the past decade an increase in terrorist attacks and the placement of hidden explosives in aircraft, transport vehicles, and public places has taken place. Detection of hidden explosives has become extremely important due to the increasing use of improvised explosive devices (IEDs) by terrorists. An IED is by definition a bomb constructed and deployed in ways other than conventional military actions. IEDs are typically fabricated in an improvised manner incorporating destructive, lethal, noxious, pyrotechnic, or incendiary chemicals and are designed to destroy or incapacitate personnel or vehicles. The majority of IEDs use conventional explosive material as their explosive load. IEDs are being used extensively against United States Military Forces and have been the cause of nearly 40% of all U.S. casualties during conflicts in the Middle East. IEDs are extremely diverse in design and are becoming increasingly sophisticated, making them difficult to detect. Several technologies have been explored to detect IEDs, but improved methods are still needed.

1.2 Prior Explosive Detection Techniques

The diversity of explosive formulations makes detection of explosives based on their chemical characteristics a challenge, but detecting hidden explosives from standoff distances of several meters or more is even more challenging. Previous and current explosive detection techniques have included a variety of methods, such as vapor detection, trained sniffer dogs, and several radiation interrogation techniques. The problem with many techniques is that they require a sample to be acquired at or near the target, which in turn puts individuals in danger.

1.2.1 Trace Detection Methods

Trace detection methods typically require a sample be taken near the target, since only trace quantities are being measured. Trace detection refers to both vapor and particulate sampling of the explosive. Trace detection equipment is passive in that it only detects the vapors or microscopic particles emitted from the explosives, as opposed to an active interrogator which typically uses a source of radiation to stimulate a response from explosives. Many common explosives have very low vapor pressures making the detection of explosive vapors difficult. Several trace detection methods are being explored; here is a brief description of some:

Chemiluminescence: Chemiluminescence is the emission of light as a result of a chemical reaction with limited emission of heat. This method is most commonly used to take evidence of blood; the sample glows upon contact with iron. The explosive detection principle is based on the detection of infrared light emitted from electronically excited nitrogen dioxide (NO_2). The reaction of nitric oxide (NO) with ozone (O_3) results in the excited NO_2. A chemiluminescence detector consists of an evacuated reaction chamber and a photomultiplier tube situated behind a red light filter. The photomultiplier tube detects the infrared light emitted from the NO_2 , with the red filter being used to block any light with spectral frequency higher than then near infrared. The amount of NO present in the reaction chamber is directly proportional to the signal output from the photomultiplier tube. It is this signal that is used to detect the presence of explosives in a chemiluminescence system. Another technology, usually gas chromatography, needs to be used before the chemiluminescence detector to separate the explosive compounds for proper identification because the chemiluminescence detector alone is not explosive-type specific. Chemiluminescence has its advantages in that it can detect a wide range of explosives, no radioactive source is required for operation, and when coupled with other technologies, has very good sensitivity and selectivity. However, the

chemiluminescence technology is typically higher in cost than other explosive detection technologies [1].

Desorption Electrospray Ionization (DESI): DESI is a method for creating ions that can be used in mass spectrometry for chemical analysis of a substance. Many explosive agents and chemical warfare stimulants have been successfully ionized using DESI. During explosive detection, DESI is carried out by directing electrosprayed charged droplets and ions of solvent onto a surface. The result of the charged particles on the surface will be the production of gaseous ions of material originally present on the surface. The ions can then be sampled with a ion trap mass spectrometer [2].

Ion Mobility Spectrometry (IMS): IMS is the process of detecting and identifying very low concentrations of chemicals based upon the differential migration of gas phase ions through a homogeneous electric field. A conventional ion mobility spectrometer consists of two main regions: a reaction region and a drift region. A collision of beta particles from a weak nickel-63 (^{63}Ni) source with nitrogen and oxygen ionizes the atmospheric pressure carrier gas (usually clean dry air) in the reaction region. Then, the explosive molecule will undergo ion/molecule reactions with the reactant ions. A mixture of reactant and product ions, under the influence of an electric field, reaches a shutter grid that separates the reaction region and the drift region. The ions are attracted to the gating grid and lose their charge due to the applied voltage bias. The grid bias is briefly turned off causing the ions to be transmitted into the drift region of the cell. The time required for ions of specific explosives to drift down the IMS tube are precisely known and are programmed into the IMS explosive detection system's microprocessor. Therefore, detecting the presence of explosive molecule ions is made possible as the microprocessor monitors the collector electrode signal at the programmed drift times [1].

Field Ion Spectrometry (FIS): Known as transverse field compensation ion mobility spectrometry, FIS is a new technique for trace gas analysis. Its principle is based on filtering ion species according to the functional dependence of their mobilities with electric field strength. FIS has been developed for trace detection of explosives, narcotics, and chemical warfare agents. This technology is quite similar to IMS in that it separates and quantifies ions while they are carried in a gas at atmospheric pressure. During operation, the sensor's ionizing cavity draws in the air sample to be analyzed. Once ionized and electrically separated from the bulk sample, the ions are carried through the spectrometer by a steady flow of clean dry air. Then, all ions except those of interest are dispersed to the sensor's walls, permitting only a select group to reach the detector. In conclusion, the detector can be tuned to selectively pass only the ions of interest, making detection of explosives and other compounds possible [1].

Immunoassay and Biosensor Methods: Immunoassay methods are based on a reaction between a target analyte and a specific antibody. A biochemical test measures the concentration of a substance in a biological liquid, using the reaction of an antibody to its antigen. During explosive detection, the sample (explosive), an enzyme conjugate of the explosive, and particles with antibodies specific to the explosive attached are mixed. Any explosives that may be in the sample and the enzyme conjugate compete for antibody binding sites on the particles. The presence of an explosive can then be detected by adding an enzyme substrate and a chromagen, creating a colored product. Biosensors use antibodies in a similar way. On fiber optic biosensors, when antibodies, immobilized on the fiber surface, bind the fluorescently labeled explosive, laser light in the evanescent wave excites the fluorophore, generating a signal. Explosives present in the sample prevent such binding and will therefore decrease the signal [2].

Photoluminescence and Semi Conducting Organic Polymers (SOP): Photoluminescence is essentially a process in which a substance absorbs photons (electromagnetic radiation) and then re-radiates photons. The use of SOPs allows

one to use photoluminescence for explosive detection. SOPs are electron-rich polymers with highly non-linear characteristics, and they bind well with molecules that have electronegative sites, such as nitrogen-rich explosives. When using SOPs for explosive detection, one uses a SOP that fluoresces when illuminated by ultraviolet light. Then, when the SOP is exposed to a certain target vapor (explosives), the vapor molecules bind to the surface of the SOP, which in turn causes a decrease in fluorescence intensity. This detected decrease in intensity indicates the presence of a certain explosive molecule [2].

The above are just a few of the many trace detection methods available. Several others are also being used to detect explosives such as: mass spectrometry, surface plasmon resonance (SPR), cavity ringdown spectroscopy (CRDS), gas chromatography, and thermo-redox [1,2]. This research aims to find a method to detect hidden explosives from safe standoff distances using a combination of both photon and neutron interrogation. To make the proposed detection method as successful as possible, it is important to understand what previous ionizing radiation interrogation techniques have been investigated.

1.2.2 Neutron Interrogation Techniques

Neutron interrogation methods generally attempt to identify explosives by their stoichiometry by performing a quantitative analysis of the contents of a target [3]. Most common explosives are composed primarily of hydrogen (H), carbon (C), nitrogen (N), and oxygen (O) and many neutron techniques can be applied to detect these HCNO compounds. Several neutron techniques include the following:

Thermal Neutron Analysis (TNA): Neutrons have excellent penetrating power in matter and interact well with nitrogen-rich materials, such as explosives, in a well known and predictable way. Several terms are used to describe the kinetic energy of a neutron, such as fast, cold, thermal, epithermal, and so forth. The term thermal neutron refers a neutron that is in thermal equilibrium wit its

surroundings. At standard room temperature, 293 K, the most probable energy of a thermal neutron is 0.025 electron volts (eV). When a thermal neutron penetrates an object and is absorbed by a nucleus, a gamma-ray photon can be emitted with an energy specific to the atom that absorbed it. The gamma-ray energies given off by atoms that capture thermal neutrons are well known and documented. During explosive detection, detecting gamma-ray photons of a known energy emitted by nitrogen after thermal neutron absorption indicates the presence of nitrogen. In turn, the number of photons detected is an indication of the amount of nitrogen present. This makes the detection of nitrogen-rich explosives possible [4].

Fast Neutron Analysis (FNA): As previously noted, neutrons have excellent penetrating power. The FNA technique is based on fast neutron interaction with matter. Explosive detection is possible with FNA by the inelastic scattering of neutrons with elements such as oxygen, carbon, and nitrogen inside the explosive. After one irradiates a target with fast, or high-energy neutrons, the fast neutrons can put nuclei of these elements in excited, short lived states. The nuclei return to their initial states by emitting radiation, often gamma-ray photons of specific energies determined by the chemical characteristics of the sample. Detecting these characteristic gamma rays makes it possible to estimate how much oxygen, carbon, and nitrogen is present with respect to each other. Determining these elemental ratios allows for the determination of the type of substance in the target. FNA has an advantage over TNA in that it is sensitive to nearly all elements in explosives, whereas TNA lacks sensitivity to two key elements in explosives, carbon and oxygen [5].

Pulsed Fast Neutron Analysis (PFNA): This technique measures the elemental composition of the contents of a scanned target. The target is scanned with a pulsed mono-energetic neutron beam, typically nanoseconds apart. The beam is created by a neutron generator, typically a deuterium-tritium (D-T) or deuterium-deuterium (D-D) reaction producing high-energy neutrons. The high-energy

neutrons interact with elements of the target and create gamma rays with energies characteristic of the elements. The energy and time of arrival of the gamma rays in the detectors allows for an elemental image of the target to be created. At this point, software is used to determine the presence of specific combinations of elements (elemental ratios), and a characterization of the target material is made [6].

Pulsed fast-thermal neutron activation analysis (PFTNA): This method is rather unique in that it utilizes both TNA and PFNA for explosive detection. To detect explosives using PFTNA, one starts by using a neutron generator to irradiate the target sample with microsecond wide fast neutron pulses; typically a D-T generator producing 14-MeV neutrons is used. During these pulses, and possibly also shortly thereafter, prompt gamma rays resulting from fast neutron inelastic scattering reactions (and nuclear reactions) are measured. Once the pulse is over, the accelerator is briefly turned off, and during this time the neutrons which have been thermalised by low atomic mass elements in the target sample can interact with elements in the sample. These interactions produce prompt capture gamma rays and can be detected just as in TNA. The cycle then starts over again. Utilizing both fast and thermal neutron analysis together in this method, one can detect characteristic gamma rays of the elements in the sample and determine the composition of the target [7].

Pulsed Fast Neutron Transmission Spectroscopy (PFNTS): During explosive detection using PFNTS, the target must be irradiated with a nanosecond pulsed broad energy neutron beam. This broad energy neutron beam is attenuated in the target sample according to the total scattering cross section of each element in the sample. Transmitted neutrons can then be detected by a bank of neutron detectors on the far side of the target. Proper analysis of the transmitted neutron spectra allows one to construct a crude map of the elements in the target sample [8].

Associated Particle Imaging (API): API is a fast neutron reaction imaging technique. In most API systems, a D-T neutron generator is used to create 14-MeV neutrons. The target sample is irradiated by this beam of fast neutrons and the neutron interaction sites can be imaged. The interactions create a neutron and an alpha particle, which move in opposite directions. Detecting the alpha particle allows the direction and time of emission of the neutron to be known. The neutron will then interact within the sample creating gamma rays to be emitted. These gamma rays can then be detected, and by measuring the time between alpha detection and gamma detection, one can determine how long the neutron traveled before reacting. One can construct a tally of these interaction sites and an image can be created of the sample [9].

Fast Neutron Scattering Analysis (FNSA): The FNSA technique consists of interrogating a target sample with a beam of fast mono-energetic neutrons, varying the neutron energy between two chosen values in the range of 3- to 8-MeV. The concept relies on detecting scattered neutrons at both forward and backward angles. In general, one can relate the detector measurements to material composition using known relationships between the scattering angle and the scattered neutron energy [10].

The above summary covered many of the neutron interrogation techniques currently used to detect hidden explosives, however, more technologies exist and more are still being developed. While neutron techniques can be effective in principle, in practice they still have some disadvantages. Photon interrogation techniques will be considered next.

1.2.3 Photon Interrogation Techniques

It is important to note at this point that both the neutron interrogation methods previously described and the photon interrogation methods about to be described are not necessarily “explosive detectors” within themselves, but rather

they are techniques that detect materials that have explosive-like characteristics. In this research, the method being utilized and described later is no different in that it uses a library of templates that are characteristic to that of an explosive to discriminate explosive materials from inert ones. Almost all traditional photon interrogation techniques make use of x rays, often times to create an image of the target sample. Explosives have unique x-ray interaction characteristics as compared to inert materials with similar elemental composition. Detecting and measuring these unique interactions can be used to identify explosives. Some common x-ray technologies include the following:

X-ray Transmission Radiography: One of the most widespread x-ray techniques used today involves x-ray transmission. The technique uses a beam of x rays penetrating the target sample to obtain an image. An x-ray beam that penetrates the target is attenuated by all objects and materials in its beam path and makes one compound image out of anything in its line-of-sight. It becomes difficult to separate the image of one object to another as more objects are added to the x-ray's beam path. This becomes particularly difficult when the target sample under investigation does not transmit or absorb x rays very well, i.e. low-atomic-number (low-Z) organics such as explosives, drugs, and plastic weapons. Dual-energy transmission systems have an advantage over single-energy systems in that material discrimination is achieved by comparing the attenuation ratio of low-energy x rays to high-energy x rays. Dual energies of around 75-keVand 150-keV are used to attempt to image low-Z organics; however, if the background is cluttered, the system is relatively ineffective [1].

Backscatter X-ray Radiography: In contrast to the traditional x-ray transmission technique, which detects high and low-Z materials by the variation in transmission through the target, backscatter x-ray radiography is a newer imaging system that detects the radiation which comes back from the target. Low-Z and high-Z materials are distinguished by their radiation scattering characteristics. Low-Z objects such as explosives, drugs, plastic weapons, and

other organic materials that typically appear low in contrast in conventional x-ray systems, appear bright white. However, detection becomes difficult if extremely dense materials are present inside the target. Low-Z objects that are behind dense material may remain hidden. AS&E has commercialized this technology and have developed what they call the Z-backscatter van. The van is a mobile imaging system that can interrogate objects, either stationary or at moderate speeds, and create a backscattered image of the target, as shown in Figure 1.1 [11].

Figure 1.1 Backscatter image taken from AS&E Z-Backscatter Van

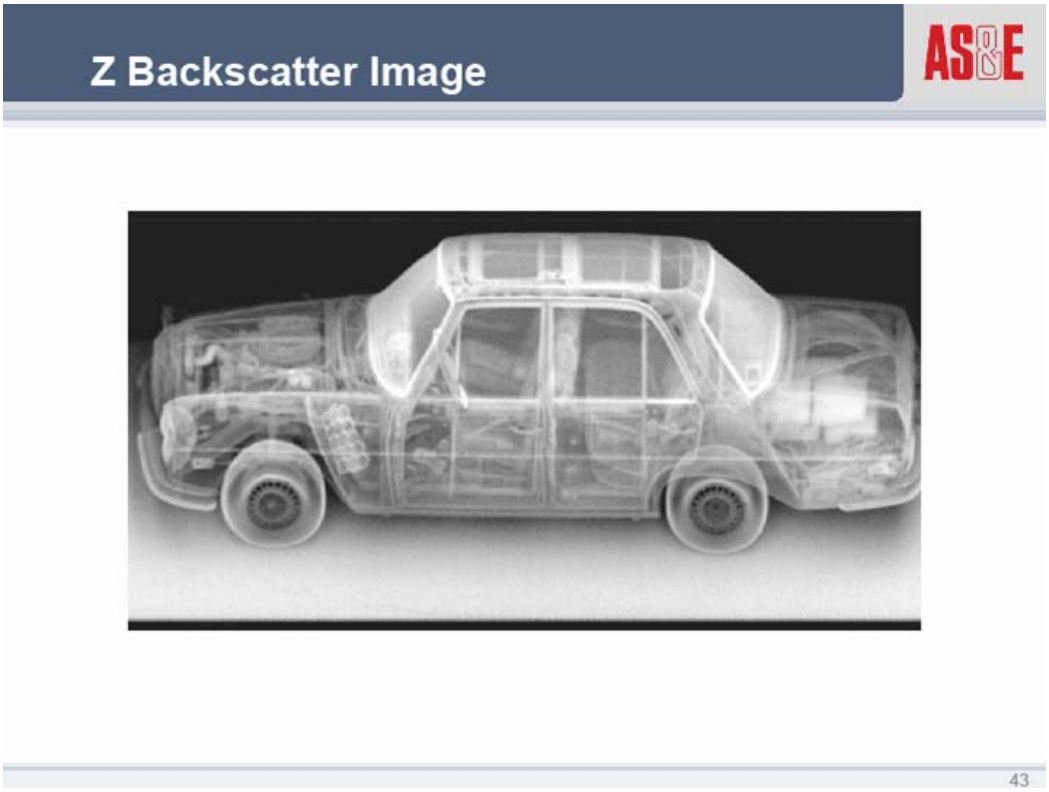

The image above is an example of how well backscatter imaging can work. However, while the image is quite useful, it measures primarily density variation at high spatial resolution with minimal information of composition. Moreover, the image must be interpreted.

Computed Tomography (CT): This method uses digital geometry processing to generate a two-dimensional image of a slice of the inside of an object. Three-

dimensional images can be obtained from a large series of two-dimensional x-ray images taken around a single axis of rotation. An x-ray beam penetrates the target and produces two-dimensional images of cross-sectional slices of an object. The three-dimensional image can then be obtained by appropriately combining a number of adjacent cross-sectional slices. CT has advantages over other imaging techniques in that it can provide very high spatial resolution and good contrast. Hence, it is useful for material detection and identification, and can be used to specifically identify explosives and discriminate them from most other inert, low-Z materials. However, while this method is quite effective, it requires that projections be collected from many different directions in order to create an accurate image [1].

Photon interrogation techniques, mainly x-ray imaging, to detect hidden explosives are some of the most frequently used methods currently being exercised. The major advantage of imaging techniques is good image resolution. However, x rays have a small interaction cross section with low-Z elements, and many organic materials such as explosive compounds and illicit drugs are composed of these low-Z elements, making discrimination between explosive and background items difficult. In addition, health risks associated with x-ray techniques must be considered.

CHAPTER 2 - Theory

2.1 Explosive Composition

Common nitrogen-rich explosives have a substantially larger ratio of nitrogen (N) to hydrogen (H), as well as a larger ratio of oxygen (O) to carbon (C), than most inert materials containing these same elements. The majority of these explosives can be characterized by a composition of about 31% nitrogen (N), 3 % hydrogen (H), 46% oxygen (O), and 20% carbon (C) [12]. The chart below gives a comparison of the amounts of H, C, N, and O in several common explosives to many common inert substances.

Figure 2.1 Atomic fractions of the elements H,C,N,O which constitute a selection of explosives, illicit drugs, and miscellaneous common substances [3].

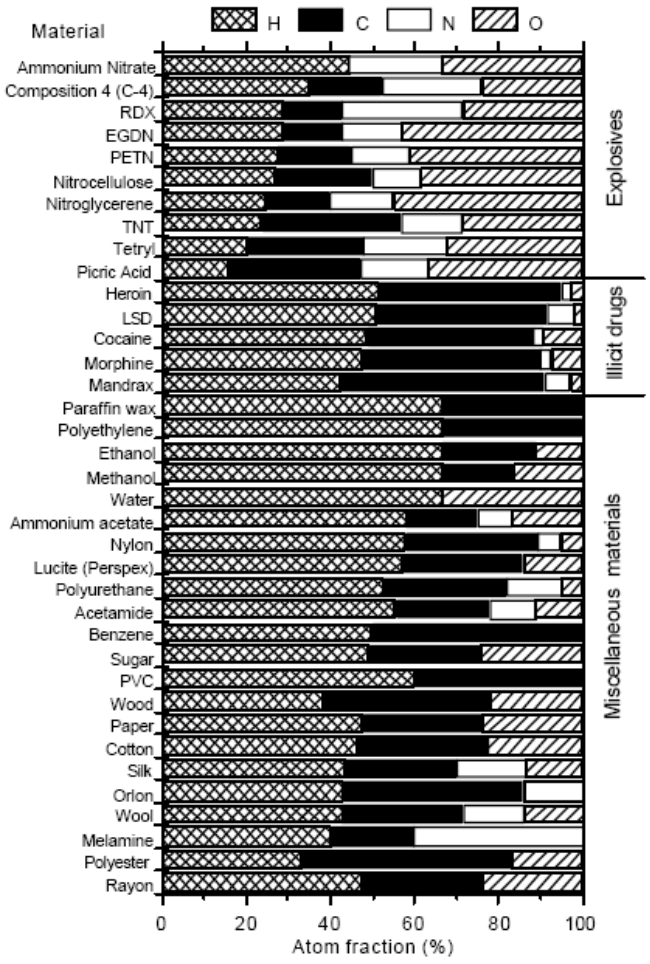

As seen from Figure 2.1, nitrogen and oxygen are the primary constituents of many HCNO explosive compounds. Most nitrogen base explosives have a nitrogen content of 31 ± 12%, with an oxygen content of 45 ± 8% [12]. The presence of over approximately 30% nitrogen and 40% oxygen in any HCNO compound almost always indicates the compound is unstable. Densities of explosives are typically over 50% higher than densities of common HCNO compounds. Similarly, other heavy materials such as metals contain elements of higher atomic number and in turn have higher densities than either explosives or common HCNO inert materials. It thus seems reasonable that it is possible to detect a significant amount of explosives in a target sample based on the presence and amount of these characteristic elements (HCNO), and the differences in densities and composition between explosives and common HCNO inert materials.

2.2 Photon Interrogation Technique

Many traditional approaches to detecting hidden chemical explosives with photons involve radiographic imaging techniques. Conventional radiographic systems that attempt to detect explosives or contraband by the use photons in the form of x rays are not sufficient. The probability of photoelectric absorption per atom behaves approximately as:

$$\tau = \frac{Z^n}{E^3} \tag{1}$$

where Z is the atomic number of the atom, E is the photon energy, and the exponent n varies between 3 for low-energy photons to 5 for high-energy photons. Therefore, the low Z-number of nitrogen-based explosives makes it difficult to distinguish them from other common materials using the photoelectric effect, on which conventional radiography relies [14].

Gamma interrogation can be used to find the density and, to some extent, the composition of a target. This technique has already been used for some time in soil sciences and the petroleum industry. Gamma-ray backscatter density gauges use the Compton scattering and photoelectric absorption of gamma-ray photons in materials to measure density and composition.

This approach can also be used to help detect hidden explosives by identifying the differences in photon signatures caused by the variations in density and composition between an explosive and an inert material. The source bombards the target with photons while the detector counts the number of backscattered photons over a wide energy range. The backscattered response essentially depends on the competition between photoelectric absorption and Compton scattering. The photoelectric cross-section increases with the atomic number of the object, while the Compton cross-section is relatively independent of the atomic number [16]. Therefore, the resulting backscattered response will favor low Z-elements of high density, such as many conventional explosives, and provide a method of detecting the differences in density, and somewhat composition, between explosive and inert materials.

The SBRS method being investigated will use multiple responses from back-streaming radiation consisting of scattered radiation and possibly 0.511-MeV photons from photon-induced positron annihilation radiation (PIPAR) as well to detect IEDs [17]. The back-streamed responses are functions not just of density (ρ), but also of average Compton (σ_C), photoelectric (σ_{pe}), and pair-production (σ_{pp}) cross sections. Pair-production occurs only when the incident gamma-ray energy is over 1.022-MeV. Interrogating a target volume will produce detector responses that are functions of some or all of these variables. Detecting the presence of an explosive is made possible by the proper analysis of these detector responses from back-streaming radiation.

Proper analysis of back-streamed detector responses is the cornerstone of the SBRS approach. The back-streamed photon interrogation responses essentially determine differences in densities, and approximate composition, of unknown targets. To accurately determine these differences and/or similarities among unknown material densities and compositions, one must have an idea of what energy range the majority of these back-streamed photons will appear in. The majority of the back-streamed photons seen by the detector in the proposed approach are Compton-scattered photons. The Compton formula is as follows,

$$E' = \frac{E}{1 + \left(E \big/ m_e c^2 \right)\left(1 - \cos \vartheta_s \right)} \tag{2}$$

where E is the initial photon energy, E' is the scattered photon energy, $\cos\vartheta_s$ is the photon scattering angle, and $m_e c^2$ is rest-mass energy of the free electron with which the incident photon collides [18]. With this formula, one can calculate the appropriate energies of the Compton-scattered photons that comprise the back-streamed responses if the initial energy of the photons interrogating the target is known, as well as the single-scatter angle, which is determined by the placement of the source and detector. Once the range of energies that the back-streamed photons appears in is known, one can then integrate the response over this range and construct the response of the unknown target. The response is then ready to be properly analyzed.

CHAPTER 3 - Analysis

3.1 Signature-Based Radiation Scanning

It is possible to detect the presence of explosives by analyzing detector responses from back-streaming radiation from interrogated target volumes. Active interrogation methods such as signature-based radiation scanning (SBRS) have advantages over passive approaches when attempting standoff explosive detection [15]. Much research is being conducted on detecting explosives, more importantly IEDs, by using active interrogation techniques with ionizing radiation. The difference in these techniques is how the target volume is interrogated and how the radiation responses are analyzed.

SBRS advantageous compared not only to passive techniques, but also to other active ionizing radiation methods such as imaging [15]. The method utilizes simple template matching from multi-dimensional information on the target as opposed to imaging methods that require very high spatial resolution. The SBRS method is a radiation-based method that can be used to detect hidden explosives by analyzing multiple radiation-induced signatures that depend on several sample variables within an interrogated volume. Typical interrogated volumes are on the order of several hundred cm^3 or larger, making spatial resolution much poorer than that for imaging techniques. However, the high resolution is not needed and the signal in this case contains much more information about the target.

The SBRS technique uses combinations of neutron and photon beams to actively interrogate a target volume. Use of neutron and photon radiation interrogation together provides more information about the target than the use of either individually. Radiation detectors record back-streaming radiation, i.e. back-scattered photons, back-scattered neutrons, prompt and inelastic-scattered gamma rays, and possibly even photon-induced positron annihilation radiation (PIPAR) [13]. The technique requires scanning the target volume in steps, recording back-streamed radiation responses at each step. These responses are not used to attempt creating an image of the target sample, but rather to use these responses for a comparison to responses from known samples. An array of detector responses **R** is collected from an unknown target. The array of responses is then compared with an explosive template **S**. The explosive template **S** is an array of detector

responses of a target in a geometric configuration known to contain explosive material. A database of explosive templates of different explosive types, different target types, in different geometric configurations can be created. One can then differentiate between targets that contain explosives and those that do not by comparing the responses from the unknown target to the library of explosive templates to construct a single figure-of-merit metric.

3.2 Figure-of-Merit Analysis

As mentioned before, the main difference between most active radiation interrogation techniques is the way in which the detector responses are analyzed. Many techniques use inversion methods to solve for the sample variables that are being sought. This involves creating mathematical models for the detector responses in terms of the target sample parameters, and then inverting the model to obtain estimates of the parameters. Depending on the complexity of the model, this inversion can be either analytic or numeric. However, with the SBRS approach, the inversion of mathematical models to obtain sample parameters such as density or composition is not necessary. It is possible to detect explosives using the SBRS method that utilizes a template-matching signature analysis. One can certainly solve the model equations to obtain estimates of the sample parameters. However, the parameters will have uncertainties associated with them since the measured responses themselves are uncertain. In turn, the process of comparing the measured parameter estimates to the desired characteristic will be subject to these uncertainties.

A template-matching technique is used here that compares a vector **R** of detector responses from an unknown target to a template **S,** which is a vector of detector responses from a similar target that is known to have explosives present. One can essentially detect the presence of a chemical explosive by creating a database of templates of different target types and geometric configurations that are known to have explosives present and comparing the response vector **R** for the specific target type to the appropriate templates.

Multiple photon beams of different energies can be used to interrogate a target from a safe, standoff distance. This will in turn create multiple back-streamed radiation

responses that can be detected. For each target type, some number L of templates can be constructed. If an explosive were present in a known configuration ℓ, then each template $\mathbf{S}_\ell = (S_{1\ell}, S_{2\ell}, \ldots, S_{N\ell})$ is the vector of N values of expected responses. One then obtains a response vector $\mathbf{R} = (R_1, R_2, \ldots, R_N)$ of N back-streamed responses by interrogating an unknown target in a similar manner. The template-matching procedure can then be applied. This procedure produces a chi-square-like figure-of-merit

$$\zeta_\ell = \sum_{i=1}^{N} \alpha_i \frac{(\beta R_i - S_{i\ell})^2}{\beta^2 \sigma^2(R_i) + \sigma^2(S_{i\ell})}, \tag{3}$$

where $\ell = (1, 2, \ldots, L)$ and α_i is a weight factor for the i^{th} signature of the form,

$$\alpha_i = \frac{w_i}{\sum_{i=1}^{N} w_i}, \tag{4}$$

with w_i being a non-negative weight for the i^{th} signature. The parameter β is a factor that scales the measured signatures to the templates, and σ^2 is the variance in the measured responses [19]. For any value of ℓ, a ζ_ℓ value less than a cut-off value, established by the user, indicates that an explosive is suspected. The cut-off value selected by the user can be modified to adjust the sensitivity and the specificity of this analysis method.

The figure-of-merit calculation has with it some uncertainty. The standard deviation of the figure-of-merit is given by [19]:

$$\sigma(\zeta_\ell) = 2\left[\sum_{i=1}^{N} \alpha_i^2 \frac{(\beta R_i - S_{i\ell})^2}{\beta^2 \sigma^2(R_i) + \sigma^2(S_{i\ell})}\right]^{1/2}. \tag{5}$$

This calculation of uncertainty is used as part of the final analysis to determine if an unknown target sample contains explosives. After the response vector **R** from the unknown target has been constructed, the figures-of-merit ζ_ℓ have been calculated, the standard deviations of the figures-of-merit $\sigma(\zeta_l)$ have been calculated, and a cut-off

value f_0 has been selected, one can then proceed toward the final analysis of discriminating explosives from inert materials.

It seems reasonable to reduce the large universe of targets into the few that are explosive, the many that are safe, and a small percentage that still are suspect. The filtering calculation is the last step in determining if an unknown target sample contains explosives. This filtering calculation will determine if a suspect target is benign, which is designated the "green" zone; is explosive, which is called the "red" zone; or requires further examination, which is designated as the "yellow" zone. The first step is to calculate the *f*-minus function:

$$f_-(\lambda_-) = \zeta - \lambda_- \sigma(\zeta). \tag{6}$$

The user can then choose a specified cut-off value f_0 as well as a value for λ. The parameter λ is adjustable and is chosen based on the confidence level one desires. If $f_-(\lambda_-) > f_0$ for all templates, then the target is considered clearly benign (green zone). If $f_-(\lambda_-)$ fails to fall in the green zone, then one proceeds to calculate f-plus as:

$$f_+(\lambda_+) = \zeta + \lambda_+ \sigma(\zeta). \tag{8}$$

If $f_+(\lambda_+) < f_0$, then the target is considered clearly an explosive (red zone). If $f_+(\lambda_+)$ fails to fall in the red zone, then it is uncertain if the target is explosive or inert and the target falls into the "yellow" zone. If a target falls into the "yellow" zone, further examination is necessary, where adjustment to the cut-off value f_0 is a possible solution.

The selection of values for f_0 and $\lambda_\pm$ is determined by the researcher, based on the sensitivity and specificity of the system and the confidence level that he or she seeks. As mentioned before, the objective is to identify as many true explosives as possible and as many true inert targets as possible, thereby minimizing the number of suspect targets. The higher the values chosen for $\lambda_\pm$, the higher the confidence in the system. For a normal distribution, choosing λ = 1 implies 68% confidence, choosing λ = 2 implies 95% confidence, and choosing λ = 3 implies 99% confidence, for either λ_+ or λ_-. The figure-of-merit equation used in this analysis has a chi-square like distribution, therefore to state that λ = 1 implies 68% confidence, λ = 2 implies 95% confidence, and choosing λ = 3 implies 99% confidence is a crude assumption. The point to be made is that the higher

the value chosen for lambda, the more confident the user is in the analysis. One could choose λ_- = 1 or 2 for good specificity (low false-positive rate) when comparing $f_-(\lambda_-)$, or one could choose λ_+ = 3 for good sensitivity (low false-negative rate) when comparing $f_+(\lambda_+)$. For example, one chooses a cut-off value of f_0 = 20 and chooses λ = $\lambda_+ = \lambda_-$ = 3 for good sensitivity and good specificity. The user then calculates a figure-of-merit value of ζ = 40 and a standard deviation of $\sigma(\zeta)$ = 5. Using the first filter to see if the target is benign one finds:

$$f_-(\lambda_-) = 40 - 3 \times 5 = 25 \tag{10}$$

It is clear to see that $f_-(\lambda_-) > 20$. Therefore, it is presumed, at the 99% confidence level, that the target is benign.

3.3 Advantages of SBRS

The SBRS approach to detecting hidden explosives is believed to have its advantages over both passive and other active interrogation methods. The SBRS approach simply seeks detection of hidden explosives and does not attempt to measure the composition of the contents of a target. The contents of a target sample are of no concern if they do not represent an explosive. Trading spatial resolution for multi-dimensional signature analysis, and the complexity of image analysis for the simplicity of template-matching, simplifies the process and allows for a quick, real-time interrogation and analysis.

The SBRS method outputs a simple yes/no result on the basis of a few figure-of-merit metrics without human interpretation being required. Human interpretation by a trained operator is only required when a target falls within the "yellow" zone. At this point further evaluation of the target may be necessary.

The SBRS procedure contains interrogation devices that can be operated remotely and from a safe standoff distance so no human operator is put in jeopardy during interrogation. Also, the components operate at standoff distances of a few meters. Thus, this method could be used for early interrogation as part of a tiered detection approach where targets with figures-of-merit below a certain cut-off would be assumed to contain

explosives while other targets could be classified as either safe or uncertain and require further investigation.

The results of this approach are based on the cumulative effect of many signatures with clutter present. It is recognized that problems associated with clutter cannot be eliminated, but they can be reduced by focusing on appropriately sized volumes, coupled with the fact that one is simply trying to determine if the signatures for any interrogated volume closely match any templates of an explosive material being in that volume. By “scanning” a target in a linear or raster-like fashion simplifies the procedure and allows one to try to detect if an explosive is present, not measure or image the contents of a target.

Lastly, new signatures can be added to this procedure at any time, making it very adaptive. We are initially investigating radiation induced signatures, but as new signatures become available they can easily become incorporated into the analysis.

CHAPTER 4 - Experimental Procedure

4.1 Equipment

The photon back-streaming experiments were conducted in the Standoff Bomb Detection Laboratory located in room 9 of Ward Hall at Kansas State University. The experiments required the use of the following:

Source: US Nuclear J-203 OCD Cobalt-60 (^{60}Co) cylindrical tube source with current activity 0.0687 Ci. ^{60}Co emits both 1.173 MeV and 1.332 MeV gamma-ray photons.

Shielding/Collimation: 2×4×8 inch lead bricks were used to construct a small box with a 2-inch square hole on one side to serve as a collimator. The box was then surrounded on the three solid sides with more lead bricks creating approximately 12 inches of shielding on each side. For some experiments a lead container with an approximately 2-inch square hole was used.

Target: Two targets were used for the experiments. The target used in the first experiment was an aluminum box. The box was constructed out of 1.588-mm (0.0625-in.) thick sheet aluminum, and is held together with screwed on angle supports. The box measures approximately 0.5 meters (20 inches) on each side with a removable lid. Inside the box, a wooden platform sitting on adjustable Unistrut angle supports was constructed to raise the samples to the appropriate height of the beam. The second target is a large suitcase in to which one-gallon paint cans comfortably fit.

Samples: One-gallon paint cans were filled with explosive surrogates and various inert materials. Four explosive surrogates were used: Ammonium Nitrate, a 30% nitrogen fertilizer which was referred to as FertA, a 36% fertilizer which was referred to as FertB, and a 50/50 mixture of FertA and FertB which was called FertAB. The various inert materials consisted of aluminum, chalk, polyethylene, rubber, sand, water, and air (empty paint can).

Computer: A Gateway personal laptop with Genie 2000 version 3.1 installed was used. Genie 2000 is a gamma-acquisition software with many powerful tools that allows the user to analyze the spectrum.

Detection System: The gamma-ray photon detector used to collect the back-streamed spectra was a Canberra 3x3 inch sodium-iodide-thallium-activated scintillation detector, NaI(Tl), model 3M3/3-X. The detector was connected to a Canberra UniSpec, serial number 11040113. The UniSpec, which connects to a computer through a USB connection, serves as a multichannel analyzer and also provides high voltage to the detector.

4.2 Experimental Setup

The setup of the equipment is an essential part to the SBRS active interrogation approach. The idea behind SBRS is to interrogate a target from a safe, standoff distance and collect back-streaming radiation from the target. Collecting back-streaming photons in an accurate and efficient way is made possible by the proper placement of the source and detector relative to the target. The setup of the equipment for the photon back-streaming experiments was the same each time. The target is placed so that the center of the target sample is two meters from the source. The collimated source of photons has a beam width of approximately 8 inches when it hits the target. The scintillation detector is placed one meter from the source and is oriented so that the front of the detector is facing the center of the target. The detector collects back-streamed photons which creates a spectrum on the computer screen. The collected back-streamed spectrum can then be integrated over a certain energy range and analyzed, providing one with a specific signature based on back-streamed photons. Figure 4.1 gives a schematic of the experimental layout.

Figure 4.1 Schematic of experimental setup with radioactive source irradiating target with unknown contents. The scintillation detector is collecting back-streamed photons.

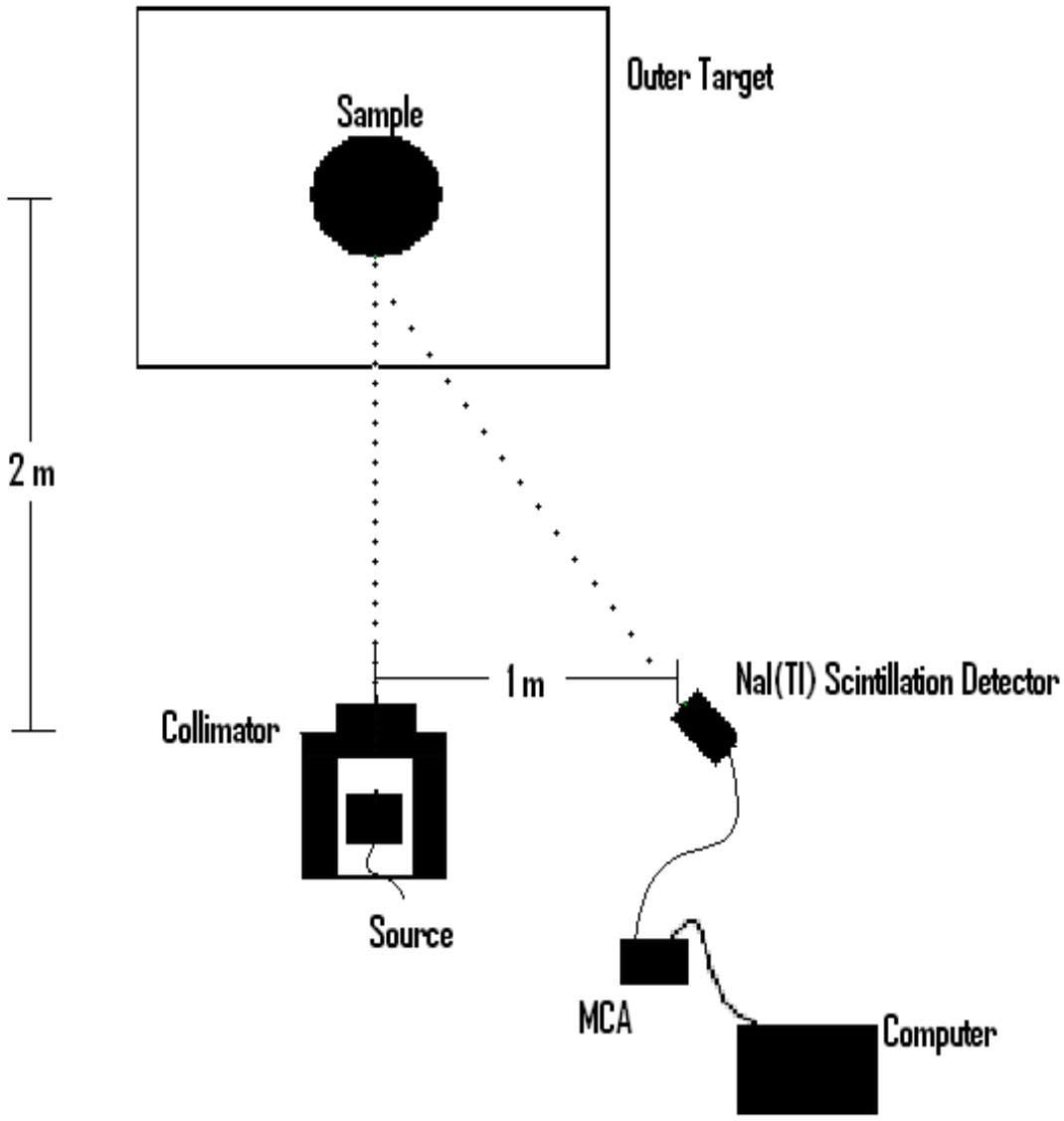

CHAPTER 5 - Results

Before any experimentation was conducted, several simulations were run using the Monte Carlo Neutral-Particle transport code (MCNP) to help determine if the SBRS approach has merit [17]. These simulation results show that by interrogation of an object with high-energy photons one can utilize the 0.511 MeV annihilation photons from PIPAR to create a particular signature. This signature is one of many that aid in the detection of hidden explosives in the overall SBRS approach. These encouraging results led the research team to believe that making use of the low-energy Compton-scattered photons from a target can also be used to create another photon signature. As mentioned before, integrating and analyzing the proper energy range of the back-streamed spectrum created by Compton-scattered photons is absolutely essential and is the main focus of this research. This was facilitated by use of the Compton formula as well as many repeatability studies to determine if the experimental results were accurate.

Knowing the initial energy of the incident photon, one can calculate approximately what energy the scattered photon will have. ^{60}Co was the radioisotope used in the back-streaming experiments. ^{60}Co emits both 1.173-MeV and 1.332-MeV gamma-ray photons, giving an average energy of approximately 1.25-MeV. Based on the placement of the scintillation detector, one can calculate the single-scatter angle of a source photon to reach the detector. This was calculated to be 153.4 degrees or 2.68 radians. Plugging these values into the Compton formula of Equation 2 yields:

$$E' = \frac{1.25}{1 + \left(1.25 \big/ 0.511\right)\left[1 - \cos(2.68)\right]} = 0.222 \text{ MeV}. \tag{11}$$

Thus, a photon with initial energy of 1.25 MeV will have approximately an energy of 0.222 MeV if it scatters through an angle of about 155 degrees. However, many photons will scatter multiple times within the target medium before reaching the detector, giving these photons even lower energies. To ensure accurate results, one wants to integrate the spectrum obtained by the detector over the proper energy range before performing the signature analysis on the data. Thus, the energy range that was decided upon was 75 to 250 keV. Integrating from 75 to 250 keV means summing all of the photons in this particular energy range to give the user a single value for **R**. Many experiments and

repeatability studies were performed to confirm that this energy range is an accurate and repeatable photon signature. Figure 5.1 shows an example spectrum taken during a photon back-streaming experiment. The *y*-axis represents the number of counts while the *x*-axis represents the corresponding energy in keV.

Figure 5.1: Response spectrum taken during photon back-streaming experiment.

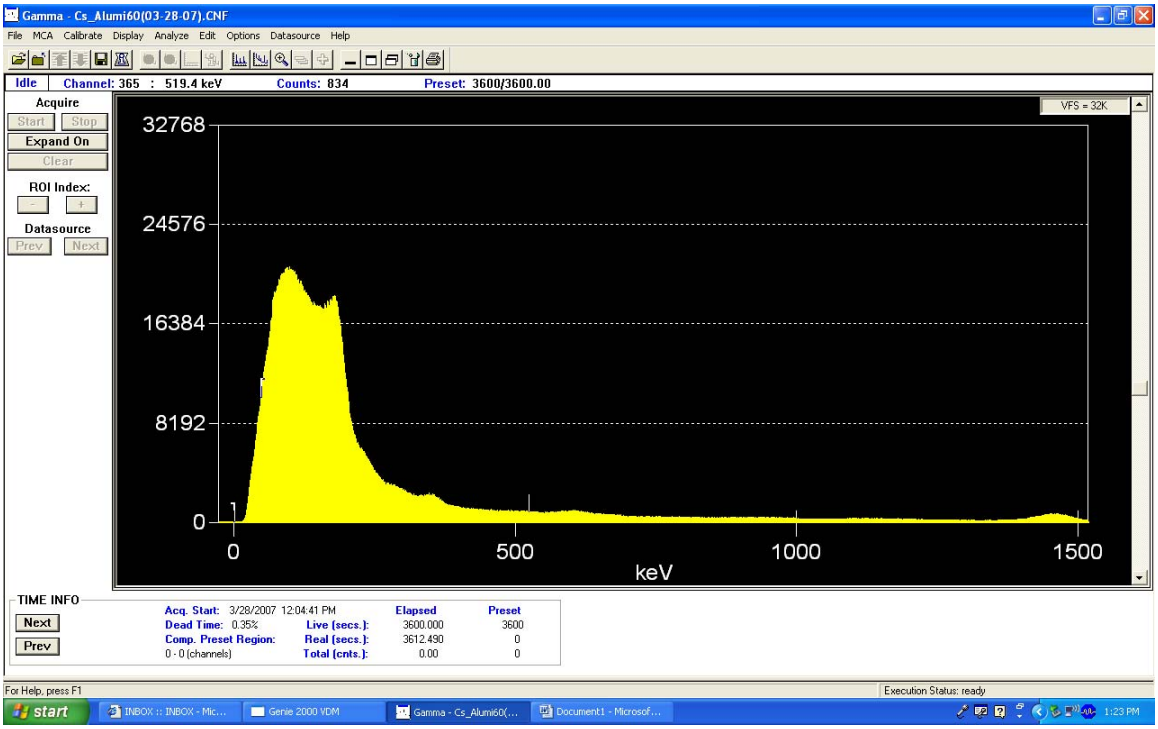

5.1 Photon Back-Streaming Experiment 1

Several experiments were conducted throughout the past two years. One of these experiments was conducted to couple the photon experimental data with data from a recently conducted neutron experiment. Three experiments that have taken place over roughly an eighteen-month period will be discussed. The first experiment reported on took place on February 21, 2007. The experimental setup for the experiment follows precisely to that of the Figure 4.1. The parameters for the experiment were as follows:

Source: ^{60}Co with activity 0.0687 Ci.

Sample size: 5-gallon

Irradiation time: 30 minutes per sample

Source, sample, and detector height: All at 40 inches from the floor

Detector: Canberra 3x3 NaI(Tl) scintillation detector with calibration title UNI1500. Details of UNI1500 can be found in Appendix 1.

Samples used: 3 explosive surrogates: FertA, FertB, and FertAB; 7 inert samples: Aluminum, Chalk, Polyethylene, Rubber, Sand, Water, and air (empty barrel)

Outer target: Aluminum box with adjustable platform

After each sample had been irradiated for the predetermined time, the back-streamed spectrum was saved as a text file. The text file contains a one dimensional array of numbers. Each number is a count associated with a corresponding channel. Using the calibration equation associated with the detector, one can convert channel number into energy. This conversion allows the user to integrate counts over a specific energy range. The experiment was conducted over a ten-hour period with no breaks except to change each sample. Each spectrum was integrated from 75 to 250 keV. The response from the FertAB sample was used as the explosive template. The goal was to discriminate the other two explosive surrogates, FertA and FertB, from the seven inert materials using FertAB as the template. For all of the photon experiments discussed here, only one photon signature was used (N = 1), the unknown responses were taken for the same amount of time as the explosive template making β = 1, and uniform weight factors were used making α = 1. Furthermore, only a single template was obtained in each experiment and thus L = 1. Finally, since each response was obtained by integrating over a contiguous energy interval, $\sigma^2(R) = R$ and $\sigma^2(S) = S$. Therefore, the figure-of-merit equation simply reduces to

$$\zeta = \frac{(R-S)^2}{R+S} \; . \tag{12}$$

For example, the user would calculate the figure-of-merit for aluminum in the following way:

$$\zeta = \frac{(661672-654778)^2}{661672+654778} = 36.104 \, . \tag{13}$$

A table of numerical responses and corresponding standard deviations for each experiment can be found in Appendix C. The results given in Table 5.1 were determined

from the experimental data. It is noted that using Equation (6), it is possible to obtain negative values of $f_{-}(\lambda_{-})$. These should merely be interpreted as indicating an explosive, since $f_0 > 0$.

Table 5.1: Results from photon back-streaming experiment 1 comparing two explosive surrogates and six inert materials to fertilizer mix template.

Sample	ζ	$\sigma(\zeta)$	$f_{-}(\lambda=3)$	$f_{-}(\lambda=2)$	$f_{-}(\lambda=1)$
Aluminum	36.104	12.017	0.052	12.07	24.087
Chalk	12.922	7.189	-8.646	-1.456	5.733
Polyethylene	109.613	20.939	46.795	67.735	88.674
Rubber	5.164	4.545	-8.471	-3.926	0.619
Sand	42.470	13.034	3.369	16.402	29.436
Water	12.890	7.181	-8.652	-1.472	5.709
Air (Empty)	436.052	41.764	310.761	352.524	394.288
			$f_{+}(\lambda=3)$	$f_{+}(\lambda=2)$	$f_{+}(\lambda=1)$
FertA	3.791	3.894	15.473	11.579	7.685
FertB	0.100	0.631	1.993	1.362	0.731

The results show that the explosive surrogates all have lower figure-or-merit values than any of the inert materials. However, to say that one can differentiate all inert materials from explosive-like materials with 99% confidence would be incorrect. Both polyethylene and air are clearly distinguishable from the explosive surrogates at the 99% confidence level, but the remainder of the inert materials are not. Setting $\lambda = 2$ and a cut-off value of f_0=12 yields much better results. At the 95% confidence level one can distinguish all but three inert materials from the explosive surrogates. Setting $\lambda = 1$ and a cut-off value of f_0=8 does not necessarily improve the results. The same three inert samples (chalk, rubber, and water) still fall below the cut-off value. While this is not ideal, one must keep in mind that this analysis was done using only one photon signature. The overall SBRS approach combines both neutron and photon interrogation for a total of as many as 10 or more signatures, depending on the number of neutron-induced

signatures used. These results are very encouraging considering only one photon signature was used and one can clearly discriminate all but three inert materials from two explosive surrogates with 95% confidence.

5.2 Photon Back-Streaming Experiment 2

The second experiment took place on April 4, 2007. The experimental setup for the experiment follows precisely to that of Figure 4.1. The parameters for the experiment were as follows:

Source: ^{60}Co with activity 0.0687 Ci.

Sample size: 5-gallon

Irradiation time: 60 minutes per sample

Source, sample, and detector height: All at 48 inches from the floor

Detector: Canberra 3x3 NaI(Tl) scintillation detector with calibration title UNI1500. Details of UNI1500 can be found in Appendix 1.

Samples used: 3 explosive surrogates: FertA, FertB, and FertAB; 6 inert samples: Aluminum, Chalk, Polyethylene, Rubber, Sand, and Water. In the interest of time, air was left out of the experiments at this point since it was always easily distinguishable from the explosive surrogates in previous experiments.

Outer target: Aluminum box with adjustable platform

The experiment was conducted over a nine-hour period with no breaks except to change each sample. Once again, each spectrum was integrated from 75 to 250 keV and the response from the FertAB explosive surrogate was used as the template. The only difference between this experiment and the first experiment described is the fact that the air (or empty barrel) sample was left out. The results in Table 5.2 were determined from the experimental data. The signatures and standard deviations obtained for this experiment are given in Table C.2.

Table 5.2: Results from photon back-streaming experiment 2 comparing two explosive surrogates and six inert materials to fertilizer mix template.

Sample	ζ	$\sigma(\zeta)$	$f_{-}(\lambda=3)$	$f_{-}(\lambda=2)$	$f_{-}(\lambda=1)$
Aluminum	15.127	7.779	-8.209	-0.431	7.348
Chalk	20.708	9.101	-6.596	2.506	11.607
Polyethylene	0.721	1.698	-4.373	-2.675	-0.977
Rubber	57.854	15.212	12.217	27.43	42.642
Sand	21.542	9.283	-6.306	2.976	12.259
Water	11.970	6.920	-8.789	-1.87	5.05
			$f_{+}(\lambda=3)$	$f_{+}(\lambda=2)$	$f_{+}(\lambda=1)$
FertA	0.451	1.344	4.483	3.139	1.795
FertB	0.385	1.242	4.111	2.869	1.627

Similar to the previous experiment, all of the inert materials have a higher figure-of-merit value than the explosive surrogates. However, one cannot clearly distinguish all of the inert materials from the explosive surrogates with 99% or 95% confidence. Using $\lambda=1$ and a cut-off value of f_0=5, one can clearly distinguish all but one inert material from the explosive surrogates with 68% confidence. Once again, this is only one photon signature, which can be coupled with back-streamed data taken from neutron interrogation to improve overall effectiveness. It is not expected to distinguish all inert materials from explosives with 95% confidence using only one photon signature.

It is important to note that while this experiment was conducted identically to that of the first experiment discussed, except for the irradiation time, there are some dramatic differences amongst the figure-of-merit values for some samples from one experiment to the next. For example, in experiment 1, polyethylene has a figure-of-merit value of 109.613 but has a figure-of-merit value of 0.721 in experiment 2. This can be explained. When using the ^{60}Co radioisotope to conduct the photon back-streaming experiments, the source had to be transferred from its original containment in the reactor bay and placed

inside the collimator in the laboratory. It was realized after several trials that the smallest misplacement of the source before starting the experiment or shifting of the source during experimentation can cause dramatic effects on the results. It was very difficult to place the source in the exact same spot inside the collimator for every experiment, thus the experimental results differ slightly from one experiment to the next. The important issue is that while source placement causes some variation in the figure-of-merit values from one experiment to the next, the same signature (range which was integrated over) was still used and reasonable results were achieved.

5.3 Photon Back-Streaming Experiment 3

The third experiment took place on February 21, 2008. The experimental setup for the experiment follows precisely to that of the Figure 4.1. The purpose of this experiment was to see how much the results changed when using a significantly smaller sample size and using a different outer target. An extra explosive surrogate was also used in this experiment. The parameters for the experiment were as follows:

Source: ^{60}Co with activity 0.0687 Ci.

Sample size: 1-gallon

Irradiation time: 30 minutes per sample

Source, sample, and detector height: All at 48 inches from the floor

Detector: Canberra 3x3 NaI(Tl) scintillation detector with calibration title UNI1500. Details of UNI1500 can be found in Appendix 1.

Samples used: 4 explosive surrogates: Ammonium Nitrate, FertA, FertB, and FertAB; 7 inert samples: Aluminum, Chalk, Polyethylene, Rubber, Sand, Water, and Air. Air was added back into the experiments by this point as someone had inquired about it being left out at a conference earlier in the year.

Outer target: Large suitcase

The experiment was conducted over a six-hour period with no breaks except to change each sample. Once again, each spectrum was integrated from 75 to 250 keV and

FertAB was the explosive surrogate used as the template. The following calculations in Table 5.3 were made from the experimental data given in Table C.3:

Table 5.3: Results from photon back-streaming experiment 3 comparing three explosive surrogates and seven inert materials to fertilizer mix template.

Sample	ζ	$\sigma(\zeta)$	$f_{-}(\lambda=3)$	$f_{-}(\lambda=2)$	$f_{-}(\lambda=1)$
Aluminum	0.969	1.969	-4.937	-2.969	-1.0
Chalk	1.419	2.383	-5.729	-3.347	-.0.964
Polyethylene	1.450	2.408	-5.774	-3.366	-0.958
Rubber	8.642	5.879	-8.996	-3.116	2.763
Sand	23.907	9.779	-5.430	4.349	14.128
Water	1.796	2.680	-6.245	-3.564	-0.884
Empty	73.881	17.191	22.309	39.499	56.690
			$f_{+}(\lambda=3)$	$f_{+}(\lambda=2)$	$f_{+}(\lambda=1)$
FertA	0.000	0.043	0.130	0.086	0.043
FertB	0.009	0.188	0.572	0.385	0.197
AmmNi	0.264	1.028	3.347	2.32	1.292

All of the inert materials have a higher figure-or-merit value than the explosive surrogates, which is very encouraging considering this experiment utilizes samples that are one-fifth the size of those used in previous experiments, and a new outer target. As in previous experiments, only a couple of inert samples are distinguishable at very high confidence levels. Decreasing the sample size affected the results slightly as not as many inert materials are clearly distinguishable at the 68% confidence level as in previous experiments. However, it is encouraging to see these results knowing that the same energy range was integrated over, the same samples (just smaller) were used, and the outer target was changed from an aluminum box to a suitcase. Discriminating the explosive surrogates from inert materials using only one photon signature is not ideal, but the results are very promising and further work is being done to couple the neutron interrogation results with the photon interrogation results to see how using multiple signatures affects the overall figure-of-merit results [19].

5.4 Photon and Neutron Interrogation Combined

It was believed that combining photon and neutron interrogation together would improve the overall effectiveness of the SBRS approach. Thus, experimental data from a neutron and a photon interrogation experiment were combined to give one combined figure-of-merit metric. The neutron experiment utilized a large aluminum box (about one meter on each side), 5-gallon samples, and a windshield placed in front the box to simulate a car. The samples were irradiated by neutrons from the tangential beam tube of the Kansas State University TRIGA Mark II reactor. The photon experiment utilized the same setup: large aluminum box, 5-gallon samples, and a windshield in front of the box. Again, ^{60}Co was the source used. Both experiments used FertAB as the explosive template. The back-streamed photon spectra were once again integrated from 75 to 250 keV to create the photon signatures (see Table C.4). The detector responses from a bare and a cadmium-covered europium doped lithium iodide (LiI(Eu)) neutron detector were used as the first two neutron signatures. The next five signatures came from neutron generated gamma-ray responses collected by a 20% efficient high purity germanium detector due to the 0.871-MeV nitrogen capture gamma ray, the 2.223-MeV hydrogen capture gamma ray, the 4.438-MeV inelastic-scatter gamma ray from carbon, the 4.945-MeV carbon capture gamma ray, and the 5.105-MeV nitrogen inelastic-scatter gamma ray, respectively (see Tables C.5-C11).

To illustrate how the results improved from using just photon or neutron interrogation alone, let us first examine the photon data by itself. Using only one photon signature, the figure-of-merits in Table 5.4 were calculated.

Table 5.4: Results from photon back-streaming experiment used to couple photon and neutron experimental data together.

Sample	ζ	$\sigma(\zeta)$	$f_{-}(\lambda=3)$	$f_{-}(\lambda=2)$	$f_{-}(\lambda=1)$
Aluminum	31.221	11.175	-2.304	8.871	20.046
Chalk	18.797	8.671	-7.216	1.455	10.126
Polyethylene	744.52	54.572	580.81	635.38	689.95
Rubber	0.653	1.616	-4.196	-2.579	-0.963
Sand	54.597	14.778	10.263	25.041	39.819
Water	413.79	40.684	291.74	332.11	373.11
Air (Empty)	215.87	29.385	127.71	157.10	186.49
			$f_{+}(\lambda=3)$	$f_{+}(\lambda=2)$	$f_{+}(\lambda=1)$
FertA	7.678	5.542	24.303	18.762	13.220
FertB	14.542	7.627	37.422	29.796	22.169

The results of this photon back-streaming experiment alone are not very desirable. It is evident that placing a windshield in front of the aluminum box to help simulate a car affected the overall results. However, this one particular photon signature does contain useful information about the target. Thus, one would expect the results to improve when coupling the photon and neutron experimental data together.

Next, the neutron experiment will be discussed. The experiment used seven overall neutron signatures. Using the detector responses from both bare and cadmium-covered europium doped lithium iodide (LiI(Eu)) neutron detectors and five signatures coming from neutron generated gamma-ray responses collected by a 20% efficient high purity germanium detector due to the 0.871-MeV nitrogen capture gamma ray, the 2.223-MeV hydrogen capture gamma ray, the 4.438-MeV inelastic-scatter gamma ray from carbon, the 4.945-MeV carbon capture gamma ray, and the 5.105-MeV nitrogen inelastic-scatter gamma ray, respectively, the results in Table 5.5 were generated. Some signatures are more useful than others; this is particularly true when doing neutron interrogation. Thus, when more than one signature is used during the analysis, the results are optimized by using weight factors to weight the signatures. For this particular

experiment, the hydrogen capture gamma-ray signature was weighted the highest $(\alpha_4 = 0.375)$, the cadmium-filtered neutron signature and the oxygen capture gamma-ray signature were weighted slightly less $(\alpha_2 = \alpha_3 = 0.2)$, the carbon 4.438-MeV signature was next with a weight of $\alpha_5 = 0.0875$, the three remaining signatures were given small weights of $\alpha_1 = \alpha_6 = \alpha_7 = 0.0125$. The weight factors were determined using a brute-force search over various permutations of weight factor values. This is achieved by holding all weight factors constant except for one signature, and then adjusting that one weight factor in 0.01 increments to see how the results are affected. Next, a different weight factor for another signature is adjusted while the remainder of the weight factors are held constant to see how that particular signature affects the results and so on and so forth.

Table 5.5: Results from neutron back-streaming experiment used to couple photon and neutron experimental data together.

Sample	ζ	$\sigma(\zeta)$	$f_-(\lambda=3)$	$f_-(\lambda=2)$	$f_-(\lambda=1)$
Aluminum	230.68	15.879	183.05	198.92	214.80
Chalk	211.32	15.269	165.51	180.78	196.05
Polyethylene	375.30	23.549	304.65	328.20	351.75
Rubber	355.34	17.711	302.21	319.92	337.63
Sand	407.71	19.943	347.88	367.82	387.77
Water	631.92	30.206	541.30	571.51	601.71
Air (Empty)	85.407	7.648	62.462	70.111	77.759
			$f_+(\lambda=3)$	$f_+(\lambda=2)$	$f_+(\lambda=1)$
FertA	4.004	1.972	9.919	7.948	5.976
FertB	9.107	2.938	17.922	14.983	12.045

The results using neutron interrogation alone are quite good. Using seven neutron signatures, one can discriminate both explosive surrogates from all seven inert materials at the 99% confidence level. However, the purpose of this exercise is to show that adding one or more photon signatures to the seven neutron signatures improves the overall

results. Using one photon signature and seven neutron signatures from both photon and neutron interrogation, we obtained the figure-of-merit metrics shown in Table 5.6. Since more than one signature was used to calculate the overall figure-of-merit, weight factors were again used to optimize the results. The hydrogen capture gamma-ray signature was weighted the highest ($\alpha_5 = 0.3$), the photon backscattered signature, the cadmium-filtered neutron signature, and the oxygen capture gamma-ray signatures were weighted slightly less ($\alpha_1 = \alpha_3 = \alpha_4 = 0.2$), the carbon 4.438-MeV signature was given a weight of $\alpha_6 = 0.07$, and the remaining signatures were given small weights ($\alpha_2 = \alpha_7 = \alpha_8 = 0.01$).

Table 5.6: Results from combining one photon and seven neutron signatures together using identical experimental setups.

Sample	ζ	$\sigma(\zeta)$	$f_{-}(\lambda = 3)$
Aluminum	190.79	12.90	152.10
Chalk	172.81	12.34	135.80
Polyethylene	449.14	21.77	383.83
Rubber	284.41	14.17	241.89
Sand	337.08	16.23	288.41
Water	588.29	25.50	511.80
Air (Empty)	111.50	8.484	86.048
	ζ	$\sigma(\zeta)$	$f_{+}(\lambda = 3)$
FertA	4.74	1.93	10.52
FertB	10.19	2.80	18.60

The results from the neutron interrogation alone were improved [19]. While some of the inert figure-of-merit values got smaller by combining photon and neutron interrogation, the difference between the smallest inert figure-of-merit value and the largest figure-of-merit value for an explosive surrogate got larger. Using a cut-off value of $f_0 = 25$ differentiates all fertilizer samples from all of the inert samples with 99% confidence. This initial trial of combining photon and neutron interrogation provides very encouraging results and future experimentation will hopefully prove this combination to dramatically improve the effectiveness of the SBRS method.

CHAPTER 6 - Conclusions

A signature-based radiation scanning approach using a template-matching analysis procedure to detect IEDs has been illustrated. Several photon back-streaming experiments have been described and the results have been promising. Using only a single photon signature, it is possible to discriminate almost all inert samples from explosive surrogates with 68% confidence. However, the sources used were not efficient at producing PIPAR, which may provide another photon-interrogation signature. It was shown that coupling neutron experimental results with photon interrogation results can improve the overall figure-of-merit results and the effectiveness of this approach. The results portrayed in this research demonstrate that photon interrogation can be used as part of a multidimensional approach to detect IEDs.

The SBRS approach has several advantages over other active interrogation methods. The method has the ability to be simple, rapid, robust, and operated at remote standoff distances. Changing the amount or placement of a material within a specific geometric configuration (clutter) will cause different responses to be produced. The SBRS technology can deal with this nonlinear effect due to clutter by investigating many different signatures and storing these templates that various clutter configurations produce.

6.1 Future Work

The SBRS approach used in an effort to detect hidden explosives, more importantly IEDs, looks very promising. However, much additional work is needed in order to make this method feasible enough to be used in the field. As mentioned before, the more signatures that can be used in this approach, the more effective and robust it will be. The sources used in photon back-streaming experiments to date are not efficient at producing PIPAR. In order for PIPAR to be produced, pair-production must occur. As mentioned before, pair-production occurs only when the incident gamma-ray photon has an energy of 1.022 MeV or greater. The cross-section for pair-production increases with gamma-ray energy, making a high-energy photon source essential for enough PIPAR to be produced to use it as an additional signature.

A 5-MeV betatron has been purchased and is currently being investigated. The betatron is a particle accelerator producing a Bremmstralung spectrum of photons with maximum energy of 5 MeV. Using a betatron has its advantages. It produces very high-energy photons and it does so with much greater intensity than the radioactive sources previously used. This results in a much smaller irradiation time which in turn produces faster results. Several studies have been done with the betatron and there are some issues that need to be addressed before this machine can be used as an effective source for future experimentation.

Future work is being planned to see how many different signatures need to be investigated and how many different explosive templates must be stored for this method to be robust enough to be used in the field. Thus, much work must be done in the future to produce the library of templates that must be created in order for this method to be successful. More experimentation is also being planned so more photon and neutron interrogation results can be combined in hopes of improving the overall effectiveness of the SBRS method, making it one step closer to a working laboratory prototype.

6.2 Recommendations

While performing my research over the past several months, several issues were encountered during experimentation. The following are a few proposed recommendations that will assist future researchers in this field of study. First, when using radioactive sources as the form of gamma-ray photons for experimentation, it is recommended to construct shielding and collimation that ensures that the source is placed in the same location each time. The smallest misplacement of the source can lead to several problems with the experimental data; more importantly the data may not be repeatable. Second, it is very important to fully understand the detection system being used during experimentation. During experimentation, a NaI(Tl) scintillation detector coupled with a UniSpec serving as the multichannel analyzer was used. Several studies were done before it was realized that the NaI(Tl) crystal is temperature dependent and a change of five to ten degrees can shift the calibration by several channels. Before starting any new experiments, it is crucial to always check the detection system to make sure everything is working properly and is consistent with previous experiments, i.e.

thoroughly check the detector calibration. Lastly, with a high-energy machine photon source being used for future photon back-streaming experiments, the use of a different photon detector is recommended. The NaI(Tl) scintillation detector currently being used is very susceptible to the high electromagnetic fields (EMF) emitted by particle accelerators. The high EMF causes a cascade of electrons in the photomultiplier tube of a scintillation detector resulting in very high detector dead times and ultimately an inefficient detector. Studies are currently being done to see if a large proportional counter can be used with a high-energy photon machine source and still provide the spectrum of back-streamed photons required for proper data analysis.

References and Bibliography

[1] D.W. Hannum, J.E. Parmeter, *Survey of Commercially Available Explosives Detection Technologies and Equipment*, National Institute of Justice, NCJ 171133, U.S. Department of Justice, 1998.

[2] A. Pettersson, S. Eallin, B. Brandner, C. Eldsater, and E. Holmgren, *Explosives Detection – A Technology Inventory*, FOI-R_2030-SE User Report, ISSN 1650-1942, 2006.

[3] A. Buffler, "Contraband Detection with Fast Neutrons," *Radiation Physics and Chemistry* **71**, 853-861, 2004.

[4] W.C. Lee, D.B. Mashood, T. Gozani, P. Ryge, and P. Shea, "Thermal Neutron Analysis (TNA) Explosive Detection Based on Electronic Neutron Generators," *Nuclear Instruments and Methods in Physics Research B* **99**, 739-742, 1995.

[5] T. Gozani, "Novel Applications of Fast Neutron Interrogation Methods," *Nuclear Instruments and Methods in Physics Research A* **353**, 635-640, 1994.

[6] D.R. Brown, A. Coates, S.N. Kuo, R. Loveman, E. Pentaleri, and R.C. Rynes, "Cargo Inspection Based on Pulsed Fast Neutron Analysis," *Proceedings of the Internaitonal Society of Optical Engineers* **2396**, 85-94, 1997.

[7] G. Vourvopoulos and P.C. Womble, "Pulsed Fast/Thermal Neutron Analysis: A Technique for Explosive Detection," *Talanta* **54**, 459-468, 2001.

[8] J.C. Overley, M.S. Chmelik, R.J. Rasmussen, R.M.S. Schofield, and H.W. Lefevre, "Explosive Detection through Fast-Neutron Time-of-Flight Attenuation Measurements," *Nuclear Instruments and Methods in Physics Research B* **99**, 728-732, 1995.

[9] E. Rhodes, C.E. Dickerman, A. DeVolpi, and C.W. Peters, "APSTNG: Radiation Interrogation for Verification of Chemical and Nuclear Weapons," *IEEE Transactions on Nuclear Science* **39**(4), 1041-1045, 1992.

[10] A. Buffler, K. Bharuth-Ram, F.D. Brooks, M.S. Allie, M. Herbert, M.R. Nchodu, and B.R.S. Simpson, "Elemental Analysis by Neutron Backscattering," *Proceedings of theInternational Socieity of Optical Engineers* **2867**, 192-197, 1997.

[11] A. Chalmers, "Single-sided X-ray Inspection of Vehicles Using AS&E's Z-backscatter Van," *Proc. SPIE* **5199**, 19-25, 2004.

[12] NRC, *Existing and Potential Standoff Explosives Detection Techniques*, National Research Council, National Academies Press, Washington D.C., 2004.

[13] G. Harding, W. Gilboy, B. Ulmer, "Photon-induced Positron Annihilation Radiation (PIPAR) – a Novel Gamma ray Imaging Technique for Radiographically Dense Materials," *Nuclear Instruments and Methods in Physics Research* A **398**, 409-422, 1997.

[14] E. Hussein, E. Waller, "Review of One-Side Approaches to Radiographic Imaging for Detection of Explosives and Narcotics," *Radiation Measurements* **29**, No. 6, pp. 581-591, 1998.

[15] W.L. Dunn, R. Brewer, K. Loschke, and J. Lowrey (2007), Radiation Interrogation Using Signature Analysis for Detection of Chemical Explosives, Proc. IEEE Conference on Technologies for Homeland Security: Enhancing Critical Infrastructure Dependability, Boston, MA, 16-17 May, 2007, pp. 7-12.

[17] W.L. Dunn, C.J. Solomon, K.W. Loschke, D.B. Bradley, W.B. Gilboy, "Ionizing Photon Methods for Standoff Bomb Detection," Nuclear Instruments and Methods in Physics Research A **580,** 778-781, 2007.

[18] J.K. Shultis, R.E. Faw, *Fundamentals of Nuclear Science and Engineering*, Marcel Dekker, Inc., New York, NY, 2002.

[19] Brewer, R.L., Dunn, W.L., 2008. "Neutron studies using the signature-based radiation scanning approach for detection of improvised explosive devices," *Nuclear Instruments and Methods in Physics Research* A (in review).

Appendix A - Detector Calibration Settings

Calibration Name: UNI1500

Calibration Equation: Energy = -28.26 + 1.494*channel + 0.00001632*channel^2

MCA Settings:

ADC: LLD = 0.89%, ULD = 100.19%, Noise = 28.24%

Stabilizer: Gain Centroid = 70 channel, Gain Mode: off

Amplifier: Fine Gain = 1.0851x

HVPS: Voltage = 875.0 volts, Polarity = positive

Appendix B - Laboratory Photo

Figure B.1: Photo of experimental setup in SBD Laboratory

Appendix C- Response Tables

Table C.1: Responses from photon back-streaming experiment 1

Sample	Response	Standard Deviation
FertAB	654778	809.2
FertA	657008	810.6
FertB	654417	809.0
Aluminum	661672	813.4
Chalk	658898	811.7
Polyethylene	666814	816.6
Rubber	652180	807.6
Sand	662257	813.8
Water	658893	811.7
Air (Empty)	631099	794.4

Table C.2: Responses from photon back-streaming experiment 2

Sample	Response	Standard Deviation
FertAB	2494627	1579.4
FertA	2496128	1579.9
FertB	2496014	1579.9
Aluminum	2503322	1582.2
Chalk	2484473	1576.2
Polyethylene	2492731	1578.8
Rubber	2477666	1574.1
Sand	2505005	1582.7
Water	2502361	1581.9

Table C.3: Responses from photon back-streaming experiment 3

Sample	Response	Standard Deviation
FertAB	2699955	1643.2
FertA	2700005	1643.2
FertB	2699737	1643.1
Ammonium Nitrate	2698761	1642.8
Aluminum	2702243	1643.9
Chalk	2702724	1644.0
Polyethylene	2697158	1642.3
Rubber	2693128	1641.1
Sand	2711329	1646.6
Water	2703070	1644.1
Air (Empty)	2680018	1637.1

Table C.4: Responses from photon back-streaming experiment used to couple photon and neutron experimental data together.

Sample	Response	Standard Deviation
FertAB	1280962	1131.8
FertA	1285401	1133.8
FertB	1287073	1134.5
Aluminum	1289921	1135.7
Chalk	1287911	1134.9
Polyethylene	1325010	1151.1
Rubber	1252256	1132.4
Sand	1292816	1137.0
Water	1313729	1146.2
Air (Empty)	1257553	1121.4

Table C.5: First neutron response (bare neutron detector) from neutron back-streaming experiment used to couple photon and neutron experimental data together.

Sample	Response	Standard Deviation
FertAB	337237	580.7
FertA	333335	577.4
FertB	341938	584.8
Polyethylene	354355	595.3
Rubber	397901	630.8
Water	313774	560.2
Sand	378537	615.3
Aluminum	341670	584.5
Chalk	357442	597.9
Air (Empty)	299308	547.1

Table C.6: Second neutron response (cadmium-covered neutron detector) from neutron back-streaming experiment used to couple photon and neutron experimental data together.

Sample	Response	Standard Deviation
FertAB	42191	205.4
FertA	42262	205.6
FertB	43856	209.4
Polyethylene	42143	205.3
Rubber	51969	228.0
Water	38906	197.2
Sand	53570	231.5
Aluminum	50345	224.4
Chalk	49484	222.4
Air (Empty)	37918	194.7

Table C.7: Third neutron response (0.871-MeV nitrogen capture gamma ray) from neutron back-streaming experiment used to couple photon and neutron experimental data together.

Sample	Response	Standard Deviation
FertAB	6187	1183.3
FertA	10119.6	37.1
FertB	5147.8	454.0
Polyethylene	4698.3	1229.3
Rubber	2337.7	37.2
Water	0.0	0.0
Sand	5010.3	1160.2
Aluminum	0.0	0.0
Chalk	5611.9	1110.1
Air (Empty)	6630.9	1081.7

Table C.8: Fourth neutron response (2.223-MeV hydrogen capture gamma ray) from neutron back-streaming experiment used to couple photon and neutron experimental data together.

Sample	Response	Standard Deviation
FertAB	7713.0	153.2
FertA	7427.8	148.8
FertB	7881.9	168.4
Polyethylene	15299.0	187.0
Rubber	10649.7	257.6
Water	16949.5	177.7
Sand	5615.6	139.3
Aluminum	5514.2	134.0
Chalk	5513.8	87.3
Air (Empty)	7627.4	240.4

Table C.9: Fifth neutron response (4.438-MeV inelastic-scatter gamma ray from carbon) from neutron back-streaming experiment used to couple photon and neutron experimental data together.

Sample	Response	Standard Deviation
FertAB	396.2	100.1
FertA	600.0	55.9
FertB	645.9	121.1
Polyethylene	784.0	128.4
Rubber	40.5	193.4
Water	404.3	98.6
Sand	988.6	122.3
Aluminum	474.7	41.4
Chalk	727.7	97.5
Air (Empty)	486.0	51.8

Table C.10: Sixth neutron response (4.945-MeV carbon capture gamma ray) from neutron back-streaming experiment used to couple photon and neutron experimental data together.

Sample	Response	Standard Deviation
FertAB	291.4	194.1
FertA	268.1	139.1
FertB	841.6	196.6
Polyethylene	532.0	38.6
Rubber	552.8	42.4
Water	441.4	35.9
Sand	770.2	46.9
Aluminum	468.4	35.3
Chalk	532.4	37.5
Air (Empty)	145.7	139.4

Table C.11: Seventh neutron response (5.105-MeV nitrogen inelastic-scatter gamma ray) from neutron back-streaming experiment used to couple photon and neutron experimental data together.

Sample	Response	Standard Deviation
FertAB	205.4	98.8
FertA	255.0	102.4
FertB	208.5	92.0
Polyethylene	46.1	105.9
Rubber	0.0	0.0
Water	0.0	0.0
Sand	0.0	0.0
Aluminum	0.0	0.0
Chalk	68.7	106.9
Air (Empty)	0.0	0.0